JOC The Journal of Organic Chemistry

Article

pubs.acs.org/joc

"Bridged" $n\rightarrow\pi^*$ Interactions Can Stabilize Peptoid Helices

Benjamin C. Gorske,* Ryan C. Nelson, Zara S. Bowden, Turner A. Kufe, and Adam M. Childs

Department of Chemistry, Bowdoin College, 6600 College Station, Brunswick, Maine 04011-8466, United States

Supporting Information

ABSTRACT: Peptoids are an increasingly important class of peptidomimetic foldamers comprised of *N*-alkylglycine units that have been successfully developed as antimicrobial agents, lung surfactant replacements, enzyme inhibitors, and catalysts, among many other applications. Since peptoid secondary structures can be crucial to their desired functions, significant efforts have been devoted to developing means of modularly controlling peptoid backbone amide *cis*−*trans* isomerism using side chains. Strategic engineering of interactions between side chain aromatic rings and backbone *cis*-amides ($n\rightarrow\pi^*_{Ar}$ interactions) is an attractive strategy for stabilizing helical structures in *N*-*a*-chiral aromatic peptoids, which are among the most utilized classes of structured peptoids. Herein, we report the first detailed computational and experimental study of $n\rightarrow\pi^*_{Ar}$ interactions in models of peptoids containing backbone thioamides, which we term "thiopeptoids". Our work has revealed that these interactions significantly affect amide rotamerism in both peptoid and thiopeptoid models via a newly characterized "bridged" mode of interaction mediated by the *N*-α-C−H σ orbitals. Overall, this work elucidates new strategies for controlling both peptoid and thiopeptoid folding and suggests that thiopeptoids will be highly structured and therefore potentially useful as therapeutics, biological probes, and nanostructural engineering elements.

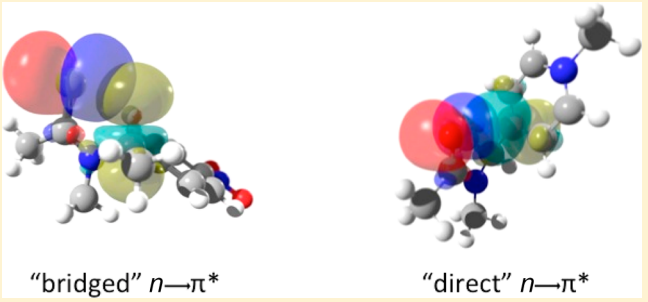

INTRODUCTION

Nature relies upon a select few classes of biopolymers such as proteins and nucleic acids to carry out a majority of the biochemical processes essential to cellular function and reproduction. The wide spectrum of chemical transformation and informational processing mediated by these biopolymers belies the limited number of monomeric building blocks typically required to achieve such diverse functions. The mechanisms by which the one-dimensional information encoded in biopolymer sequences gives rise to biological complexity have enthralled researchers in the fields of biochemistry, molecular biology, and chemistry for decades. Chemists in particular have been inspired to develop artificial polymers that might harness the inherent advantages of modular molecular assembly in order to mimic the functions of biological molecules. Peptides and proteins were especially attractive early targets for mimicry, as they can often function independently of other cellular machinery. The development of peptide mimics such as β-peptides[1−3] and peptoids,[1,3−5] along with many classes of polypeptide isosteres,[1,3−13] heralded the emergence of the field of peptidomimetics, which has grown rapidly since its inception. The more broadly defined term "foldamer"[1,3−5,12,14] was later introduced in recognition of the fact that peptidomimetic design principles can also be employed to construct abiotic folded structures, which have potential applications in materials design, nanoengineering, and molecular computing.

Peptoids, which are polymers of *N*-substituted glycine, are an increasingly important class of foldamers due to their biostability, facile synthesis, and structural diversity (Figure 1A).[1−13] These advantages have recently spurred the expansion of the peptoid family to include oligomers such as β-peptoids[15−19] and azapeptoids.[20,21] Although peptoids were originally designed to be rapidly accessible via combinatorial chemistry, specific subclasses of peptoids and their congeners have also been shown to fold predictably into discrete structures.[22−31] Recent advances in understanding this folding have catalyzed interest in the rational design of peptoid secondary and tertiary structures and have aided the develop-

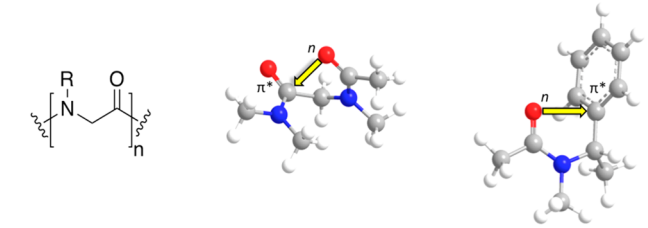

Figure 1. (A) Generic peptoid structure. (B) 3D-representations of $n\rightarrow\pi^*_{Am}$ and (C) $n\rightarrow\pi^*_{Ar}$ interactions (indicated by yellow arrows) in peptoid model systems that stabilize the *trans*- and *cis*-rotamers, respectively.

Received: June 29, 2013
Published: September 19, 2013

   dx.doi.org/10.1021/jo4014113 | J. Org. Chem. 2013, 78, 11172−11183

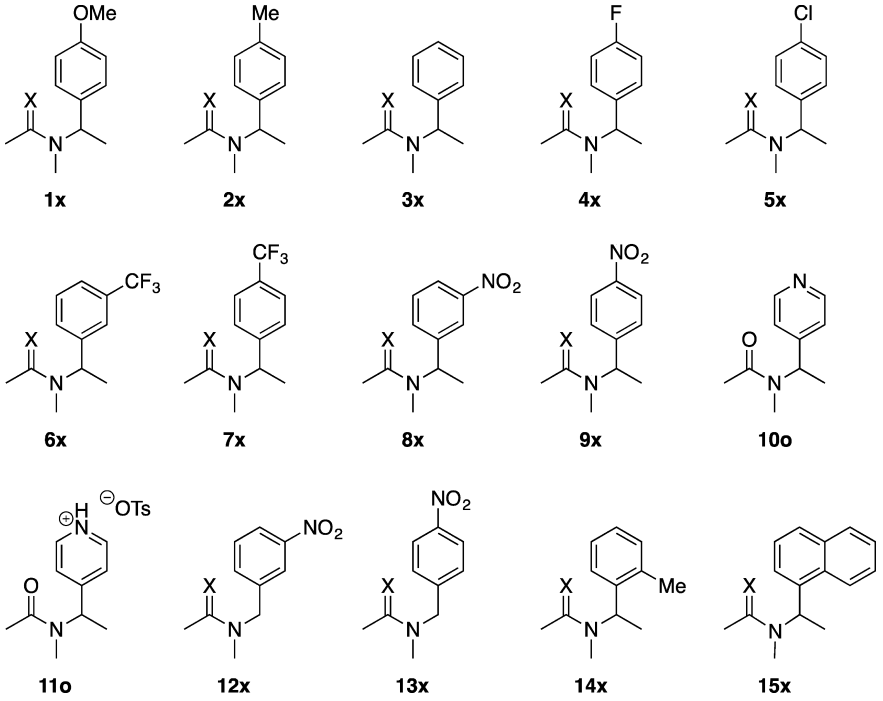

Figure 2. Structures of the peptoid (X = O; **1x**–**15x** with **x** = O) and thiopeptoid (X = S; **1x**–**15x** with **x** = S) model compounds examined in this study.

ment of peptoids as therapeutic agents,[5,32−38] catalysts,[39] and nanostructural elements.[40−44]

Peptoids containing *N*-α-chiral aromatic side chains constitute perhaps the most utilized class of structured peptoids to date.[24,31,37,45−47] Despite lacking hydrogen bond donors and stereogenic centers in their backbones, early computational work suggested that *N*-α-chiral peptoids could adopt a helical structure analogous to a polyproline type I (PPI) helix, which is comprised entirely of *cis*-amides;[22] these predictions were later borne out by circular dichroism, nuclear magnetic resonance, and X-ray crystallography studies.[24,25,45,48] A "threaded loop" structure stabilized by hydrogen bonds and containing several *trans*-amides can also predominate for certain *N*-α-chiral aromatic peptoids;[47,49,50] this finding highlights how a few relatively weak noncovalent interactions can dramatically affect the secondary structures of this peptoid class. Indeed, the small differences in energy between the *cis*- and *trans*-rotamers of the tertiary amides in the peptoid backbone typically lead to an undesirable ensemble of interconverting structures in solution.[48]

Since the helicities of *N*-α-chiral aromatic peptoids have been correlated to their functions in many applications,[5,34,37,46,51] considerable effort has been devoted to developing strategies for limiting their conformational heterogeneity by promoting helical structure. Head-to-tail cyclization[26] and "stapling" together proximal side chains within the helix[52] have proven to be very successful approaches in this regard. Alternatively, directing the *cis*–*trans* isomerism of specific backbone amides using their pendant side chains holds a particular appeal due to its complete compatibility with the powerful and facile "submonomer" peptoid synthesis protocol.[27,28,30,31,49,53,54] Moreover, the ability to modularly and rationally "program" rotameric propensities for specific peptoid backbone amides simply by the choice of side chain would represent a powerful methodology for the design of new, nonhelical peptoid structures. Previous work along these lines has revealed how peptoid backbone amides can interact with each other via an "$n\rightarrow\pi^*_{Am}$ interaction" similar to that observed in polyprolines (Figure 1B).[53−55] This interaction entails the delocalization of electron density from a donor amide lone pair into the π^* orbital of a neighboring amide. Importantly, the requirement that this interaction occur along the Bürgi-Dunitz trajectory dictates that it can only lower the energy of the *trans*-rotamer of the donor amide. A complementary interaction between a peptoid backbone amide and π^* orbitals of an electron deficient aromatic ring in the side chain (an "$n\rightarrow\pi^*_{Ar}$ interaction") has been shown to stabilize the *cis*-rotamer of the donor amide (Figure 1C).[53,54] The usefulness of this interaction in stabilizing *cis*-amides was recently demonstrated in peptoids containing a triazolium side chain that serves as a junction to additional side chain constituents attached using click chemistry.[56]

We reasoned that advancing our understanding of $n\rightarrow\pi^*_{Ar}$ interactions could aid the development of new strategies for controlling peptoid amide isomerism and thereby peptoid secondary structure. While the electrophilicity of the aromatic ring has previously been investigated in this context, the nucleophilicity of the amide donor has not been as extensively examined thus far.[57] Inspired by reports that related $n\rightarrow\pi^*_{Am}$ interactions in prolines and β-peptoid models can be strengthened using thioamide donors,[57,58] we sought to determine whether thioamide analogs of α-peptoids, which we have dubbed "thiopeptoids", could also engage in stronger $n\rightarrow\pi^*_{Ar}$ interactions.

Herein we report our experimental and computational studies of peptoid and thiopeptoid model systems in which both the $n\rightarrow\pi^*_{Ar}$ interaction donor and acceptor are systematically probed. Our analyses of these systems have elucidated a new "bridged" mode of $n\rightarrow\pi^*_{Ar}$ interaction that is facilitated by a *N*-α-C−H σ^* orbital, and that operates concurrently with the previously reported "direct" mode of $n\rightarrow\pi^*_{Ar}$ interaction. Our data suggest that this bridged mode of $n\rightarrow\pi^*_{Ar}$ interaction can play a considerable role in determining $K_{cis/trans}$ for amides and

dx.doi.org/10.1021/jo4014113 | J. Org. Chem. 2013, 78, 11172−11183

Table 1. Peptoid (1o−15o) and Thiopeptoid (1s−15s) Model Systems (Figure 2), Amide and Thioamide *Cis*/*Trans* Ratios in $CDCl_3$ ($K_{cis/trans}$)[a] and Corresponding Free Energy Differences ($\Delta G_{cis/trans}$)[b,c]

		oxoamide			thioamide		
side chain designation	σ[a]	entry	$K_{cis/trans}$[b]	ΔG[d] (kcal/mol)	entry	$K_{cis/trans}$[b]	ΔG[d] (kcal/mol)
p-OMe	−0.27	**1o**	1.95 ± 0.03	−0.39	**1s**	1.99 ± 0.05	−0.41
p-Me	−0.17	**2o**	1.72 ± 0.01	−0.32	**2s**	1.77 ± 0.01	−0.34
p-H	0	**3o**	1.8[e]	−0.34	**3s**	1.9	−0.39
p-F	0.06	**4o**	2.57 ± 0.06	−0.56	**4s**	2.72 ± 0.04	−0.59
p-Cl	0.23	**5o**	2.73 ± 0.07	−0.59	**5s**	2.80 ± 0.05	−0.61
m-CF_3	0.43	**6o**	3.13 ± 0.06	−0.67	**6s**	3.4 ± 0.1	−0.73
p-CF_3	0.54	**7o**	3.24 ± 0.07	−0.70	**7s**	3.2 ± 0.1	−0.69
m-NO_2	0.71	**8o**	4.31 ± 0.05	−0.86	**8s**	4.8 ± 0.1	−0.93
p-NO_2	0.78	**9o**	4.2[e]	−0.85	**9s**	5.1	−0.96
4py		**10o**	3.5	−0.74	NA[f]	NA	
4pyH+		**11o**	10.1 ± 0.7	−1.4	NA	NA	
m-NO_2 pm	0.71	**12o**	2.65 ± 0.06	−0.58	**12s**	3.1 ± 0.1	−0.67
p-NO_2 pm	0.78	**13o**	2.73 ± 0.08	−0.58	**13s**	2.95 ± 0.09	−0.64
o-Me	NA	**14o**	3.71 ± 0.07	−0.78	**14s**	3.84 ± 0.03	−0.79
1ne	NA	**15o**	10.4 ± 0.3	−1.4	**15s**	14.6 ± 0.5	−1.6

[a]Hammett substituent constant; see ref 65. [b]Determined by integrating ^{1}H NMR spectra of 15 mM solutions in $CDCl_3$ at 24 °C. Data ranges indicate standard error, when applicable. [c]Single stereocenters do not influence $K_{cis/trans}$ in these systems; enantiomeric excesses were therefore not determined. The *cis*-rotamer was defined as that which orients the side chain and the oxygen/sulfur atom on the same side of the amide/thioamide bond (see Figure 3A). [d]$\Delta G = -RT \ln(K_{cis/trans})$. [e]Previously reported in ref 53. [f]Data not available.

thioamides in the backbones of peptoids and thiopeptoids, respectively. The backbone side-chain interactions observed in thiopeptoids suggest that thiopeptoid oligomers will be capable of adopting robust PPI helix structures with at least comparable conformational stability and homogeneity relative to typical α-peptoids. We also explore the tactical disruption of bridged $n\rightarrow\pi^*_{Ar}$ interactions that could potentially lead to the formation of new peptoid secondary structures containing *trans*-amides. Overall, these interactions constitute a new architectural element for constructing highly structured peptoids and thiopeptoids that could serve as potent antimicrobial agents,[37] enzyme inhibitors, and ligands of proteins and nucleic acids,[59,60] as well as components of higher order foldameric structures such as helix bundles.[42,43]

RESULTS AND DISCUSSION

Density Functional Theory (DFT) Calculations of Conformational Energies for 3o, 9o, and 16o. Computational modeling is a powerful tool for investigating weak interactions, so we initiated our investigations of $n\rightarrow\pi^*_{Ar}$ interactions in peptoids and thiopeptoid models by calculating the conformational energies of previously reported peptoid models **3o** (containing an unsubstituted aromatic ring) and **16o** (containing an *N*-methylpyridinium ring) using DFT methods (Figure 2, Table 1, Figure 3A).[53] Compound **16o** was previously shown to exhibit a very high *cis*−*trans* amide ratio, such that the *trans*-rotamer is nearly undetectable by ^{1}H NMR. ^{1}H nuclear Overhauser effect (NOE) spectroscopy indicated that the *cis*-rotamer (*cis*-**16o**) favors a conformation in which the amide oxygen and the *ipso* carbon are in close proximity ($C_{amide}-N_{amide}-C_{benzyl}-C_{ipso}$ dihedral angle between −75° and +75°; Figure 3B), suggesting the influence of a strong, direct $n\rightarrow\pi^*_{Ar}$ interaction. In contrast, NOE data suggested that this conformation was not extensively populated in compound **3o**. Constrained geometry potential energy surface (PES) scans of the $C_{amide}-N_{amide}-C_{benzyl}-C_{ipso}$ dihedral angle (Figure 3) for both amide rotamers of **16o** corroborate these previous experimental results (Figure 4). Plots of the computed energies

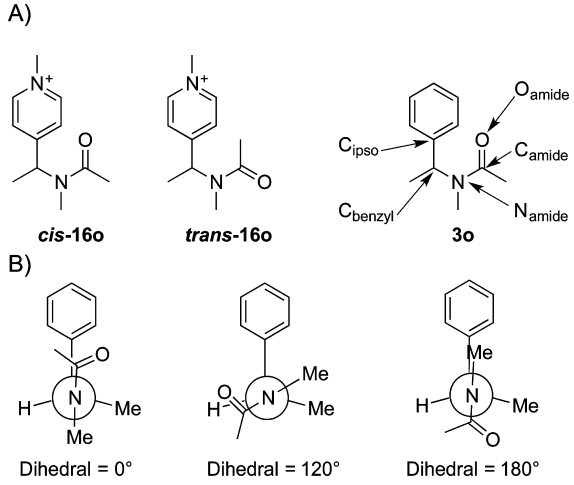

Figure 3. (A) Structures of the *cis*- and *trans*-rotamers of a previously reported peptoid model containing an *N*-methylpyridinium group in its side chain and the corresponding phenyl analogue with relevant atomic labels. (B) Newman projections of conformations of **3o** with $C_{amide}-N_{amide}-C_{benzyl}-C_{ipso}$ dihedral angles of 0°, 120°, and 180°.

(relative to those of the global minima) and $C_{ipso}-O_{amide}$ interatomic distances as functions of the dihedral angle suggest that a strong direct $n\rightarrow\pi^*_{Ar}$ interaction indeed stabilizes the *cis*-amide rotamer of **16o**. Specifically, the calculated global minimum for compound **16o** corresponds to a conformation in which the $C_{amide}-N_{amide}-C_{benzyl}-C_{ipso}$ dihedral angle is near −50°, giving a $C_{ipso}-O_{amide}$ interatomic distance that is shorter than the sum of the carbon and oxygen van der Walls radii (3.22 Å). In contrast, a similar conformation in which this direct $n\rightarrow\pi^*_{Ar}$ interaction can occur represents only a local minimum for **3o** (Figure 4B), with the calculated global minimum corresponding to the conformation in which the amide carbonyl and *N*-α-C−H bonds are roughly eclipsed ($C_{amide}-N_{amide}-C_{benzyl}-C_{ipso}$ dihedral angle near 120°; Figure 3B). This conformation is reminiscent of those adopted by

dx.doi.org/10.1021/jo4014113 | J. Org. Chem. 2013, 78, 11172−11183

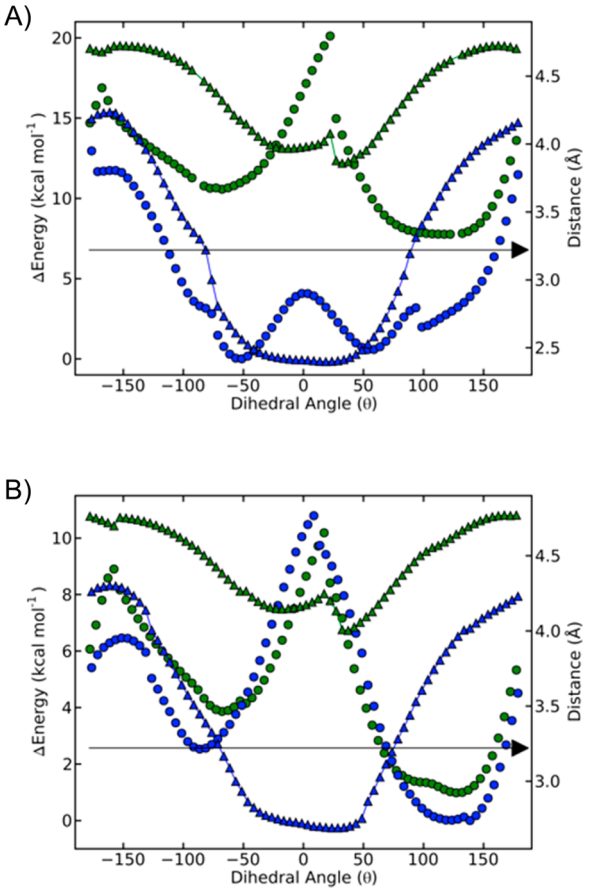

Figure 4. Computed energies (left axis, circles) and $C_{ipso}-O_{amide}$ interatomic distances (right axis, triangles) for *cis*- (blue) and *trans*- (green) rotamers of **16o** (A) and **3o** (B) as functions of the $C_{amide}-N_{amide}-C_{benzyl}-C_{ipso}$ dihedral angle. Energies are reported relative to the global minima of the dihedral scans. Dihedral angles are defined as shown in Figure 3. The horizontal arrow shows the distance at which the carbon and oxygen atoms make contact as defined by the sum of their van der Waals radii (3.22 Å).

proline residues within the α-helices of proteins and is consistent with the operation of 1,3-allylic strain. [61] However, the stabilization of this conformation has also been attributed in part to a Cα−H···O═C interaction.[62,63] Although such interactions are typically referred to as conventional, purely electrostatic hydrogen bonds, contributions from weak covalent interactions between the amide π system and the Cα−H bond have also been suggested. [62] This same interaction has recently been shown to significantly affect proline *cis*−*trans* isomerism in a model peptide.[64] Most importantly, the geometric arrangements of atoms required for this interaction pervade the previously reported solution-phase and solid-state structures of peptoid PPI-like helices and are consistent with NOE spectroscopy data for compound **3o** (vide infra).[25,31,48] In addition, a thiopeptoid model compound with an *N*-α-naphthyl side chain has been shown to adopt a similar conformation in the solid state that would facilitate a Cα—H···S═C interaction.[57] Notably, natural bond orbital (NBO) calculations suggested that the *cis*-amide rotamers of peptoids and thiopeptoids with *N*-α-naphthyl side chains are also stabilized by a C−H···O═C interaction between the carbonyl oxygen and an aromatic hydrogen.

We sought to assess the relative contributions of direct $n\rightarrow\pi^*_{Ar}$ and C−H···O═C interactions to amide *cis*−*trans* isomerism in *N*-α-chiral aromatic peptoids as functions of the electrophilicity of the side chain aromatic ring. We began by performing a dihedral scan for both amide rotamers of compound **9o**, which contains a *para*-nitroaromatic ring that we surmised to be of intermediate electrophilicity compared to those of **3o** and **16o** (Figure 5A). As expected, a local minimum

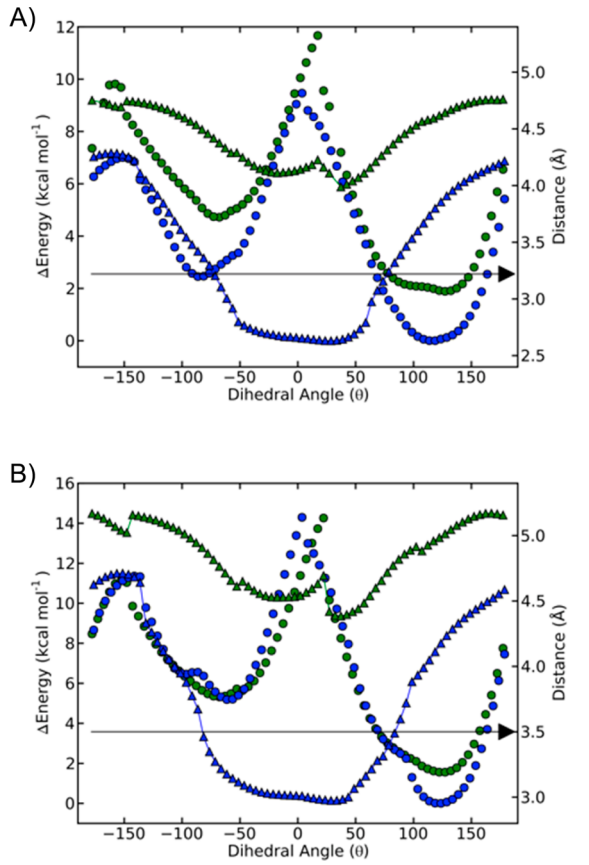

Figure 5. Computed energies (left axis, circles) and $C_{ipso}-O/S_{amide}$ interatomic distances (right axis, triangles) for *cis* (blue) and *trans* (green) isomers of **9o** (A) and **9s** (B) as a function of $C_{amide}-N_{amide}-C_{benzyl}-C_{ipso}$ dihedral angle. Energies are reported relative to the global minimum of the dihedral scan. The dihedral angles are defined as shown in Figure 3. The horizontal arrow shows the distance at which the C_{ipso} and O/S_{amide} atoms make contact, as defined by the sum of their van der Waals radii (3.22 Å for oxygen, 3.50 Å for sulfur).

occurs near the point where the $C_{ipso}-O_{amide}$ interatomic distance dips below the sum of the van der Waals radii, suggesting that a direct $n\rightarrow\pi^*_{Ar}$ interaction contributes to lowering the energy of *cis*-**9o**. However, we were intrigued to find that the global minimum again corresponds to the conformation in which the amide carbonyl and the *N*-α-C−H bonds are roughly eclipsed. Furthermore, the difference in energy between the global minima of the *cis* and *trans* rotamers of **9o** is larger compared to that for **3o**, commensurate with the larger $\Delta G_{cis/trans}$ for **9o** as compared to **3o** that was previously observed experimentally.[53] These energy differences are not readily attributable to 1,3-allylic strain, since both **9o** and **3o** are calculated to adopt essentially identical global minimum conformations while exhibiting notably different *cis*/*trans* ratios.

Determination and Analysis of $K_{cis/trans}$ for Peptoid and Thiopeptoid Models. In order to investigate the relative contributions of electrostatic vs weak covalent interactions to

dx.doi.org/10.1021/jo4014113 | J. Org. Chem. 2013, 78, 11172−11183

the calculated global minimum conformations of **3o** and **9o**, we synthesized a series of peptoid models in which the electrophilicity of the *N*-α-chiral aromatic ring was systematically altered (Table 1). We then synthesized thiopeptoid analogs of these models in order to probe how the nucleophilicity of the $n\rightarrow\pi^*_{Ar}$ donor affects $K_{cis/trans}$. Thioamides are useful probes of electrostatic and weak covalent attractions, as the thioamide sulfur is less negatively polarized as compared to the oxygen of an amide, while concomitantly exhibiting heightened nucleophilicity that enhances covalent interactions.[58] Therefore, significantly lower $K_{cis/trans}$ values would be expected if the global minimum conformation were stabilized primarily by electrostatic interactions involving the thioamide sulfur, while higher $K_{cis/trans}$ values would indicate such interactions are significantly covalent in nature. Notably, these model systems do not contain additional amides, and thus preclude the interference of amide−amide "$n\rightarrow\pi^*_{Am}$" interactions previously observed in peptoids and polyprolines. Regardless, such backbone−backbone interactions are weaker than the competing backbone-side chain interactions in homologous dimeric peptoid models.[53−55,57] While neither the electron density in the aromatic ring nor the nucleophilicity of the donor chalcogen (oxygen or sulfur) correlate with the observed *cis-trans* ratios ($K_{cis/trans}$) for neutral or electron-rich aromatic rings (**1**−**3**), $K_{cis/trans}$ increases markedly as the electrophilicity of the ring is increased (**4**−**9**). Furthermore, the differences between the $\Delta G_{cis/trans}$ values for the oxoamides and the corresponding thioamides (Table 1) increase as the electrophilicity of the aromatic ring increases, consistent with a primarily covalent, as opposed to electrostatic, interaction dictating $\Delta G_{cis/trans}$ A paired *t* test of the complete $K_{cis/trans}$ data set confirmed that the thioamide model systems exhibited statistically significant increases in $K_{cis/trans}$ compared to the analogous peptoid models. In addition, previous studies have shown that $\Delta G_{cis/trans}$ values for most α-chiral *aliphatic* peptoid model systems are typically near or even greater than zero;[54,66] thus, interactions involving the α-chiral *aromatic* side chains of our model systems are likely the primary source of stabilization of the *cis*-rotamer over the *trans*-rotamer. In light of these observations, we hypothesized that an orbital-controlled covalent stabilization of the global minimum conformation identified above for *cis*-**3o** and *cis*-**9o** (Figures 4 and 5) becomes more significant as the electron density in the ring is decreased.

Identification and Analysis of a "Bridged" $n\rightarrow\pi^*_{Ar}$ Interaction. In order to corroborate this hypothesis and identify the most important weak covalent interaction affecting $\Delta G_{cis/trans}$ in these systems, we opted to perform NBO calculations, as these can offer an intuitive, localized orbital perspective of such interactions.[67] In particular, NBO second-order perturbation (SOP) energies are indicative of the importance of filled-to-empty NBO interactions in structural stabilization, and thus provide a means of identifying weak covalent interactions. We first calculated NBO SOP energies for the global minima of the *cis*- and *trans*-rotamers of **9s** identified in a dihedral scan (Figure 5B). Since a large number of SOP interactions for each rotamer were identified, we first focused on interactions that were significantly perturbed upon *cis-trans* isomerization (i.e., exhibited large "$\Delta E(\mathrm{SOP})_{cis/trans}$" values). We then discounted groups of interactions that changed in a self-compensatory manner upon isomerization such that their net contribution to the calculated $\Delta E_{cis/trans}$ was negligible (see the Supporting Information). We reasoned that the remaining interactions would be the most important contributors to $\Delta G_{cis/trans}$. Of these, the interaction calculated to be affected most significantly by *cis-trans* isomerization of **9s** is that between a sulfur lone pair and the σ^* orbital of the *N*-α-C−H bond (Figure 8.) The significance of this interaction is remarkable in light of the poorer spatial overlap of these orbitals in thioamides as compared to amides due to the longer C═S vs C═O bond. (The offsetting of this poorer orbital overlap with enhanced donor nucleophilicity in the thioamide vs amide model systems may play a role in producing the similarity in $K_{cis/trans}$ values for **1o**−**3o** vs **1s**−**3s**.) We inferred that the loss of this interaction upon *cis-trans* isomerization would most significantly affect $K_{cis/trans}$ in *N*-α-chiral thiopeptoids. Notably, the *N*-α-C−H bonding NBO is in turn calculated to interact with the π-system of the aromatic ring (see the Supporting Information). We thus conjectured that the overall trend of increasing $K_{cis/trans}$ with increasing ring electrophilicity for **1**−**9** might be best be explained by an increasingly favorable "bridged" $n\rightarrow\pi^*_{Ar}$ interaction, in which the $n\rightarrow\pi^*_{Ar}$ electron density shift is mediated by the *N*-α-C−H σ^* orbital (Figure 6). According to this central hypothesis, the

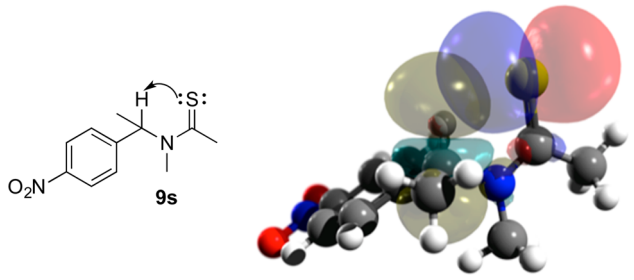

Figure 6. 2D and 3D representations of the interaction between a lone pair NBO on the thioamide sulfur atom of **9s** (red and blue) and the *N*-α-C−H σ^* NBO (yellow and green), which could serve as a "bridge" for electron density transfer from the thioamide sulfur atom to the electron-deficient aromatic ring.

N-α-C−H σ^* orbital effectively serves as a conduit for electron density transfer from the chalcogen lone pair to the electrophilic aromatic π system. To further validate this hypothesis, we examined the changes in the NBO SOP interactions between the (thio)amide chalcogen donor and the *N*-α-C−H σ^* acceptor for peptoid models **1o**−**9o** and thiopeptoid models **1s**−**9s**. The calculated strengths of the putative bridged $n\rightarrow\pi^*_{Ar}$ interactions in these models correlated exceedingly well with both the calculated $\Delta E_{cis/trans}$ (see the Supporting Information) and the experimentally determined $\Delta G_{cis/trans}$ (Figure 7) values. Subsequent analysis of the SOP interactions in these models likewise implicated this same interaction as the primary contributor to $\Delta G_{cis/trans}$ (see the Supporting Information). Although weaker than the Cα−H···O═C interactions in polyprolines, which have estimated energies of 1.2—3.6 kcal/mol,[63] the energies of these bridged $n\rightarrow\pi^*_{Ar}$ interactions (greater than 0.65 kcal/mol for electron deficient systems **6**−**9**) are considerable in light of the inherent flexibility of the peptoid backbone and are comparable to hydrogen bonds. Moreover, since peptoid helix formation has been shown to be cooperative,[23] bridged $n\rightarrow\pi^*_{Ar}$ interactions may contribute more significantly to peptoid structural stability than suggested by the single interaction energies.

In order to obtain further experimental evidence for bridged $n\rightarrow\pi^*_{Ar}$ interactions in our model compounds, we measured the $^1J_{CH}$ coupling constants for the *N*-α-C−H bonds of the *cis*-

dx.doi.org/10.1021/jo4014113 | J. Org. Chem. 2013, 78, 11172−11183

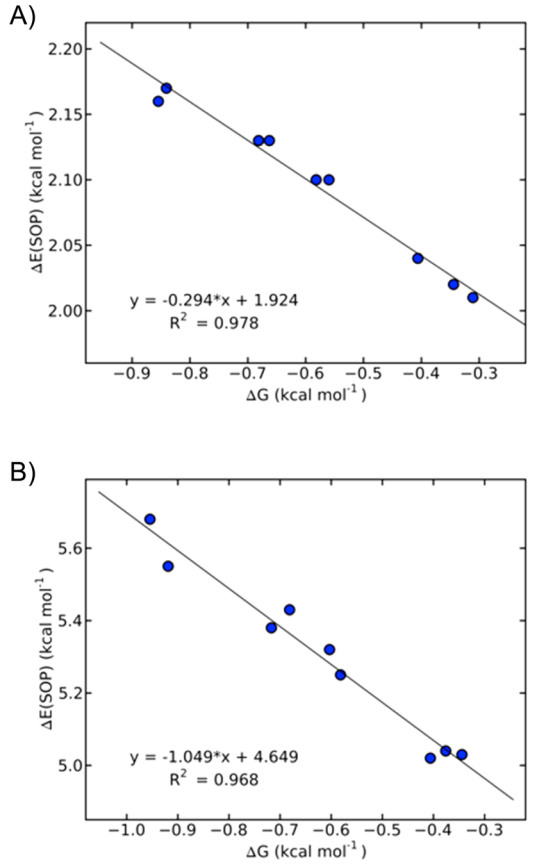

Figure 7. Calculated $\Delta E(\mathrm{SOP})_{cis/trans}$ values for the interaction between the (thio)amide chalcogen lone pair and the *N*-α-C−H σ^* orbital in oxoamide (A) and thioamide (B) model compounds, plotted against the experimentally determined $\Delta G_{cis/trans}$ values for each compound (Table 1).

Table 2. Experimentally Measured $^1J_{CH}$ Coupling Constants for the *N*-α-C−H Bonds of the *Cis*- and *Trans*-Rotamers of Selected Model Compounds

			N-α-C−H $^1J_{CH}$		
compd	side chain designation	σ^a	*cis*	*trans*	Δ^1J_{CH}
1o	*p*-OMe	−0.27	137.9	134.7	3.2
9o	*p*-NO_2	0.78	141.1	137.5	3.6
9s	*p*-NO_2	0.78	139.4	136.6	2.8
10o	4py		140.6	136.4	4.2
11o	4pyH+		139.5	ND[b]	
13o	*p*-NO_2 pm		138.4	138.4	0

[a]See ref 61. [b]Rotamer not detected.

and *trans*-rotamers of selected molecules (Table 2). Increases in this coupling constant have been cited previously as evidence of C−H···O interactions.[68−70] A larger $^1J_{CH}$ coupling constant was detected for the *cis*- vs the *trans*-rotamer of each compound except **13o**, while *cis*−*trans* isomerization did not affect any other measurable $^1J_{CH}$ coupling constants. Furthermore, the magnitudes of $^1J_{CH}$ for the *cis*-rotamers roughly correlate with the observed $K_{cis/trans}$ values. Intriguingly, $^1J_{CH}$ for *cis*-**11o** containing a protonated, pyridinium side chain was *lower* than that for the neutral pyridine-containing *cis*-**10o**, suggesting that the bridged $n\rightarrow\pi^*_{Ar}$ interaction plays a lesser role in determining $K_{cis/trans}$ for *cis*-**11o**. This finding supports both our calculations (vide supra) and previously reported solution phase NMR data that implicate the direct mode of $n\rightarrow\pi^*_{Ar}$ interaction as the primary determinant of $K_{cis/trans}$ in peptoids containing pyridinium rings in their side chains.[53] Overall, these data suggest that the bridged $n\rightarrow\pi^*_{Ar}$ interaction is the primary mode of chalcogen-to-aromatic electron density transfer in *cis*-*N*-α-chiral aromatic peptoids containing electron-rich, neutral, and moderately electron-poor aromatic rings, while the direct mode of $n\rightarrow\pi^*_{Ar}$ interaction dominates for *cis*-*N*-α-chiral aromatic peptoids containing highly electron-deficient aromatic rings.

A similar transition from the bridged to direct mode of $n\rightarrow\pi^*_{Ar}$ interaction also appears to occur in the thiopeptoid models. Hammett plots for these compounds deviate from linearity at high σ values, suggesting that the mechanism of *cis*-rotamer stabilization changes as the side chain aromatic rings become highly electron deficient (see the Supporting Information). In order to better understand this phenomenon, we performed constrained geometry PES scans of the $C_{amide}-N_{amide}-C_{benzyl}-C_{ipso}$ dihedral angle (Figure 3) for both thioamide rotamers of **9s** (Figure 5B) and compared them to those of the oxo-analogue **9o** (Figure 5A). As the C_{ipso}−chalcogen interatomic distances dip below the sum of the van der Waals radii near the −75° dihedral angle, the conformational energies of *cis*-**9o** increase while those of *cis*-**9s** decrease in a manner similar to that calculated for *cis*-**16o**, which exhibits a favorable direct $n\rightarrow\pi^*_{Ar}$ interaction. These calculations thus imply that a direct $n\rightarrow\pi^*_{Ar}$ interaction, though not occurring in the global minimum conformation, plays a more important role in dictating $K_{cis/trans}$ for **9s** vs **9o**; this hypothesis is supported by the lower $^1J_{CH}$ and smaller Δ^1J_{CH} observed for *cis*-**9s** as compared to *cis*-**9o**. Given that both modes of $n\rightarrow\pi^*_{Ar}$ interactions are as strong or stronger in thiopeptoid vs peptoid models containing electron-deficient aromatic rings, the former foldamer class could exhibit a strong propensity to form *cis*-thioamides and PPI-type helices.

Disruption of $n\rightarrow\pi^*_{Ar}$ Interactions Using Peptoid and Thiopeptoid Side Chains. We also tested our hypothesis that bridged $n\rightarrow\pi^*_{Ar}$ interactions play an important role in determining $K_{cis/trans}$ in peptoid and thiopeptoid models by synthesizing model compounds in which both the thermodynamic and kinetic stabilities of the conformations engendering the interactions were altered. Compounds **12** and **13** lack an *N*-α-methyl group but are otherwise identical to **8** (*m*-NO_2) and **9** (*p*-NO_2), respectively. We expected that this change would reduce steric interactions and thereby *lower* the energies of alternate conformations (in which the bridged $n\rightarrow\pi^*_{Ar}$ interaction could not occur) and the rotational barriers leading to them, resulting in a weakening of the bridged $n\rightarrow\pi^*_{Ar}$ interaction as evidenced by a lower $K_{cis/trans}$. This supposition was borne out by the experimental data for **12** and **13** (Table 1), which show an overall lowering of $K_{cis/trans}$ for the compounds lacking an *N*-α-methyl group. Moreover, the magnitude of $^1J_{CH}$ for *N*-α-C−H bond in the *cis*-rotamer of **13o** is indistinguishable from that of the *trans*-rotamer (Table 2). These data suggest that the lower $K_{cis/trans}$ values for **12** and **13** are due in part to a weaker bridged $n\rightarrow\pi^*_{Ar}$ interaction in these systems, and are not entirely dictated by the reduced sizes of the side chains.

We also synthesized derivatives of **3** containing either an *o*-methyl group (**14o** and **14s**) or a naphthyl ring (**15o** and **15s**) designed to *increase* steric interactions and rotational barriers. Interestingly, while the *o*-methyl group significantly increased $K_{cis/trans}$ in **14o** compared to **3o**, thionation did not result in any

dx.doi.org/10.1021/jo4014113 | J. Org. Chem. 2013, 78, 11172−11183

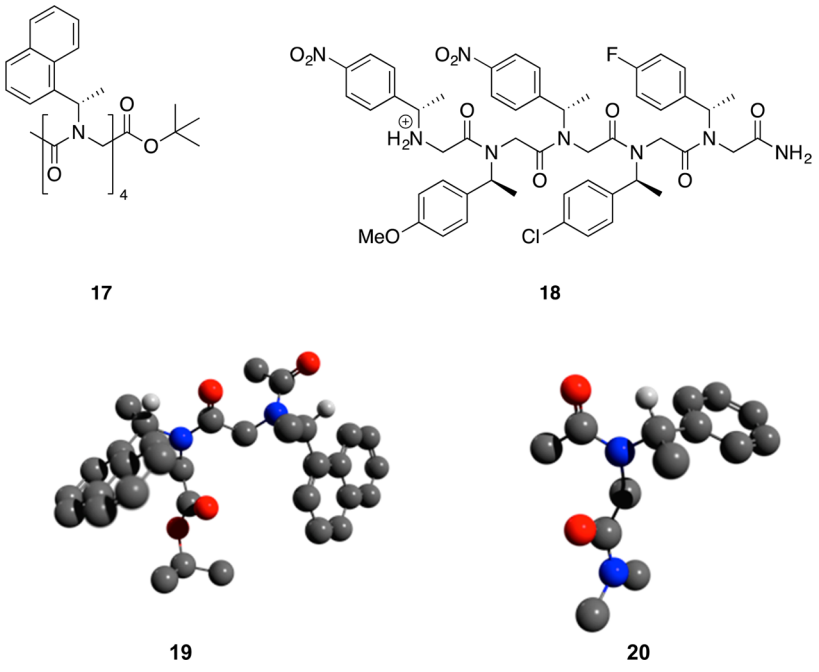

Figure 8. Structures of polypeptoids reported to form helices in the solid state (**17**) and in solution (**18**) and the geometry-optimized subunits used for calculating the energies of the bridged $n\rightarrow\pi^*_{Ar}$ interactions in each compound (**19** and **20**; gray = carbon, blue = nitrogen, red = oxygen, white = hydrogen; most hydrogen atoms removed for clarity).

further increase. In contrast, **15o**, in which a naphthyl ring carbon is attached at the *ortho*-position, exhibited a larger $K_{cis/trans}$ value vs **3o**; this difference was also amplified in the thionated analog **15s**. We therefore speculate that *o*-alkyl substitution of *N*-α-chiral side chains simply increases their effective steric bulk, leading to larger $K_{cis/trans}$ values. While the large $\Delta\Delta G_{cis/trans}$ observed for the compounds containing the naphthyl (1ne) side chain (**15o** and **15s**) could be due in part to strong $n\rightarrow\pi^*_{Ar}$ interactions in *cis*-**15o** and *cis*-**15s** that are enhanced by conformational restriction, a recently elucidated naphthyl C−H···O═C interaction could also play a significant role in these systems.[57]

Evidence of Bridged $n\rightarrow\pi^*_{Ar}$ Interactions Contributing to Polypeptoid Structure. Examination of previously reported solution- and solid-phase structures of peptoid helices strongly suggests that the bridged $n\rightarrow\pi^*_{Ar}$ interactions affecting $K_{cis/trans}$ in our monomeric models play an important role in the folding of polypeptoids as well. Inspection of the helical solid-state structure of **17**[31] and the solution-phase structure of **18**[48] (which notably contains a preponderance of electron-deficient α-chiral aromatic side chains) reveals that the conformation of each interior monomer unit closely corresponds to the calculated global minimum conformations of **1**−**9** in which the bridged $n\rightarrow\pi^*_{Ar}$ interaction can occur (Figure 8). To determine if bridged $n\rightarrow\pi^*_{Ar}$ interactions might similarly operate within these polypeptoid helices as in our model systems, NBO calculations were performed on geometry optimized subunits (**19** and **20**) of the helices. (The geometry optimizations had little effect on the overall structures but were necessary to ensure that experimental structural metrics were not significantly affected by model simplification.) The bridged $n\rightarrow\pi^*_{Ar}$ SOP interaction energies were calculated to be −1.73 kcal/mol and −1.92 kcal/mol for **19** and 2.18 kcal/mol for **20**; these energies are in line with those determined for our model systems. Furthermore, the fact that the $n\rightarrow\pi^*_{Ar}$ SOP interaction energies in **20** are larger than those in the analogous monomeric models highlights the potentially cooperative nature of these types of interactions in stabilizing the secondary structures of peptoid oligomers. Thus, given that the reported $K_{cis/trans}$ equilibria for most α-chiral *aliphatic* peptoid model systems are typically near unity,[54,66] the bridged $n\rightarrow\pi^*_{Ar}$ interactions facilitated by α-chiral *aromatic* side chains in these helices could play a significant role in dictating both amide isomerism and, thereby, overall folding. Indeed, early peptoid structural studies demonstrated that incorporation of electron-deficient α-chiral aromatic side chains, which have been shown above to enhance bridged $n\rightarrow\pi^*_{Ar}$ interactions, amplified circular dichroism signatures associated with peptoid helices.[23]

SUMMARY AND CONCLUSIONS

Our computational and experimental studies of chalcogen−aromatic interactions in models of *N*-α-chiral aromatic peptoids and thiopeptoids suggest that $n\rightarrow\pi^*_{Ar}$ interactions can operate in two distinct modes: either via a direct $n\rightarrow\pi^*_{Ar}$ interaction between the amide or thioamide and the aromatic ring, or via a newly characterized "bridged $n\rightarrow\pi^*_{Ar}$" mode of interaction in which electron density transfer from the amide/thioamide to the aromatic ring is facilitated by an intermediary *N*-α-C−H σ^* orbital. Although both interaction modes are calculated to operate to some extent within the compounds examined in this study, the latter mode appears to be most significant for electron-rich, neutral, and moderately electron-poor aromatic side chains, while the former mode increasingly affects *cis*−*trans* isomerism in compounds containing more strongly electron-deficient aromatic side chains. Both interaction modes are calculated to be enhanced by electron-deficient aromatic side chain acceptors and thioamide donors, and stabilize the *cis*-rotamer of the proximal backbone amide or thioamide. Thus, these interactions could potentially be exploited to construct robust PPI-type helices useful in a wide range of applications. Importantly, although the C−H···O═C interaction component

dx.doi.org/10.1021/jo4014113 | J. Org. Chem. 2013, 78, 11172−11183

of the bridged $n\rightarrow\pi^*_{Ar}$ interaction has previously been observed to affect proline *cis-trans* isomerism,[64] peptoids and thiopeptoids present a unique opportunity to modulate the strength of this interaction via readily incorporated *N*-α-chiral aromatic side chains. Although beyond the scope of this study, the intentional disruption of these $n\rightarrow\pi^*_{Ar}$ interactions might allow other weaker interactions to play a more dominant role in controlling amide/thioamide isomerism, potentially leading to the formation of new structures containing *trans*-rotamers.

In addition, we have conducted the first detailed study on the conformational preferences of thiopeptoid monomers. This work provides an important foundation for predicting and understanding the folding of *N*-α-chiral aromatic thiopeptoids. Although the synthesis and structural characterization of polythiopeptoids is ongoing in our laboratory, it is as yet unclear how the subtle balance of weak interactions that operate to direct peptoid amide isomerism will differ from that in thiopeptoids. Given that thioamides have already been shown to engage in enhanced $n\rightarrow\pi^*_{Am}$ interactions as compared to their oxo-counterparts,[58,71] we postulate that stabilization of both *cis*- and *trans*-rotamers by rational design might be readily orchestrated in thiopeptoids. Our findings, in conjunction with this previous report, suggest that thiopeptoids and mixed peptoid/thiopeptoid oligomers would constitute a fundamentally new and manipulable class of peptidomimetics, and that they could find numerous applications in medicine, materials design, and chemical biology. Current efforts in our laboratory are dedicated to realizing the potential of polythiopeptoids in these areas, focusing on the construction of biomimetic structures such as PPII-type helices that could be used to interrogate protein−protein interactions.

EXPERIMENTAL SECTION

General Methods. Unless otherwise noted, all reagents were 99% purity, ACS-grade or HPLC-grade. Thin-layer chromatography (TLC) was performed on glass silica gel plates, 250 μm, with UV254. TLC plates were visualized using an ultraviolet lamp and heat-activated staining with potassium permanganate, ceric ammonium molybdate, and *p*-anisaldehyde.

Instrumentation. All ^{1}H nuclear magnetic resonance (NMR) spectra were collected on a 400 MHz NMR spectrometer. All samples were prepared in $CDCl_3$, unless otherwise noted. Chemical shifts were recorded in parts per million (ppm), using tetramethylsilane (TMS) as the 0.0 ppm reference, unless otherwise noted. ^{13}C NMR spectra were obtained using ^{1}H-broadband decoupling.

High-resolution mass spectrometric analysis was performed using a quadrupole time-of-flight (Q-TOF) mass analyzer, equipped with a nanoelectrospray ionization (nanoESI) source. Chromatographic separation and nanoESI was performed using a 40 nL enrichment column and a 43 mm × 75 μm analytical column, both packed with 300 Å, 5 μm particles with C18 stationary phase. The mobile phases were 0.1% formic acid/H_2O (A) and 0.1% formic acid/acetonitrile (B). Samples were loaded using 98:2 (A/B) and eluted using a linear gradient with 30:70 (A/B) at 12 min. Mass spectra were collected in positive ion mode; spectra were internally calibrated using methyl stearate ($C_{17}H_{35}CO_2CH_3$) and hexakis(1*H*,1*H*,4*H*-hexafluorobutyloxy)phosphazine (HP-1221; $C_{24}H_{18}O_6N_3P_3F_{36}$), continuously introduced and detected as $[M + H]^+$.

Synthesis and Characterization of Model Peptoids and Thiopeptoids. Model peptoids **1o**−**15o** (Figure 2, Table 1) were synthesized using previously reported procedures[53,54] or using a one-pot reductive amination protocol (Scheme 1). Thiopeptoid model compounds **1s**−**15s** (Figure 2, Table 1) were prepared from the corresponding peptoid models using Lawesson's reagent. All compounds were purified to homogeneity by silica gel chromatography. Absolute configurations and enantiopurities were not germane to this study and therefore were not determined. Peptoid model systems **3o**, **9o**, **10o**, and **13o** were synthesized as previously reported.[53,54] Full characterization data for model systems **1o**−**8o**, **12o**, **14o**, **15o**, **1s**−**9s**, and **12s**−**15s** are provided below. After purification, a 15 mM solution of each compound in $CDCl_3$ was prepared and a ^{1}H NMR spectrum was obtained using a relaxation delay of 35 s. $K_{cis/trans}$ values were determined by comparing the integrations of the *cis*- and *trans*-rotamer peaks in the ^{1}H NMR spectra. Reported data ranges for $K_{cis/trans}$ correspond to standard errors for these sets of measurements, when applicable. Proton-coupled ^{13}C NMR spectra were obtained using gated decoupling experiments.

Scheme 1. One-Pot Synthesis of Peptoid Model Compounds

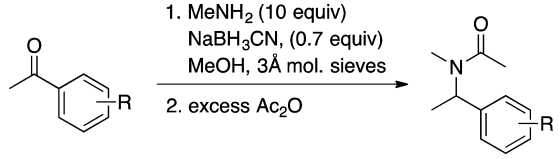

Representative Model Peptoid Synthesis (3o; Scheme 1). To a dry 25-mL flask were added 4 Å molecular sieves, a magnetic stirring bar, 2 M methylamine in methanol (16.7 mL, 33.3 mmol), acetophenone (388 μL, 3.33 mmol), and sodium cyanoborohydride (146 mg, 2.33 mmol). The reaction mixture was stirred under nitrogen for 48 h. The solution was then cooled to 0 °C, and acetic anhydride (2.3 mL, 33.3 mmol) was added dropwise to the stirred solution. After 5 min, the solution was placed in a separatory funnel, ethyl acetate (25 mL) was added, and the organic layer was washed with aqueous 10% citric acid (25 mL), saturated aqueous sodium bicarbonate (25 mL), and saturated aqueous sodium chloride (25 mL). The organic layer was dried over magnesium sulfate and filtered. Removal of the solvent in vacuo yielded pure *N*-methyl-*N*-(1-phenylethyl)acetamide (384 mg, 67% yield) as a colorless oil.

Representative Model Thiopeptoid Synthesis (9s).[58] To a dry 50-mL round-bottom flask were added *N*-methyl-*N*-(1-(4-nitrophenyl)ethyl)acetamide (574 mg, 2.58 mmol), 15 mL of dry tetrahydrofuran, a magnetic stirring bar, and Lawesson's reagent (522 mg, 1.29 mmol). The reaction mixture was refluxed for 15 h, after which the reaction was allowed to cool to room temperature and then quenched with 1 N HCl (1 mL). The resulting mixture was extracted with ethyl acetate (3 × 15 mL), and the combined organic layers were washed with saturated aqueous sodium bicarbonate (50 mL) and saturated aqueous sodium chloride (50 mL). The organic layer was dried over magnesium sulfate, filtered, and concentrated in vacuo to yield a brown oil. The oil was purified by silica gel chromatography (100% *n*-hexanes to 100% ethyl acetate gradient) to give **9s** (428 mg, 50% yield) as a yellow solid. Model peptoid **9s** was fully characterized; see below.

***N*-(1-(4-Methoxyphenyl)ethyl)-*N*-methylacetamide (1o).** Aqueous workup yielded 212 mg (54% yield) of *N*-(1-(4-methoxyphenyl)ethyl)-*N*-methylacetamide as a clear oil with sufficient purity such that column chromatography was not required: TLC R_f = 0.1 (2:1 hexanes/EtOAc); ^{1}H NMR (400 MHz, $CDCl_3$; major rotamer) δ 7.16 (AA′BB′, J = 8.9 Hz, 2H), 6.86 (AA′BB′, J = 8.8 Hz, 2H), 6.02 (q, J = 7.0 Hz, 1H), 3.80 (s, 3H), 2.63 (s, 3H), 2.12 (s, 3H), 1.45 (d, J = 7.1 Hz, 3H); ^{13}C NMR (100 MHz, $CDCl_3$; major rotamer) δ 170.2, 158.5, 132.4, 128.2, 113.5, 55.0, 49.3, 29.7, 22.0, 13.9; HRMS m/z $[M + H]^+$ calcd for $C_{12}H_{18}NO_2$ 208.1332, found 208.1329.

***N*-Methyl-*N*-(1-(*p*-tolyl)ethyl)acetamide (2o).** Silica gel chromatography (3:1 diethyl ether/chloroform) yielded 246 mg (29% yield) of *N*-methyl-*N*-(1-(*p*-tolyl)ethyl)acetamide as a clear oil: TLC R_f = 0.45 (3:1 ether/chloroform); ^{1}H NMR (400 MHz, $CDCl_3$; major rotamer) δ 7.21−7.11 (m, 4H), 6.03 (q, J = 7.1 Hz, 1H), 2.64 (s, 3H), 2.33 (s, 3H), 2.12 (s, 3H), 1.45 (d, J = 7.2 Hz, 3H); ^{13}C NMR (100 MHz, $CDCl_3$; major rotamer) δ 170.6, 170.5, 137.7, 137.3, 136.9, 129.5, 129.2, 127.3, 126.4, 55.2, 53.6, 49.8, 30.2, 27.7, 22.4, 21.5, 21.1,

dx.doi.org/10.1021/jo4014113 | J. Org. Chem. 2013, 78, 11172−11183

21.0, 17.7, 15.7; HRMS m/z $[M + H]^+$ calcd for $C_{12}H_{18}NO$ 192.1383, found 192.1195.

***N*-(1-(4-Fluorophenyl)ethyl)-*N*-methylacetamide (4o).** Silica gel chromatography (3:1 diethyl ether/chloroform) yielded 463 mg (59% yield) of *N*-(1-(4-fluorophenyl)ethyl)-*N*-methylacetamide as a white crystalline solid: mp 87−88 °C; TLC R_f = 0.5 (3:1 ether/chloroform); ^{1}H NMR (400 MHz, $CDCl_3$; major rotamer) δ 7.27−7.19 (m), 7.10−6.99 (m), 6.05 (q, J = 7.1 Hz, 1H), 2.65 (s, 3H), 2.13 (s, 3H), 1.46 (d, J = 7.1 Hz, 3H); ^{13}C NMR (100 MHz, $CDCl_3$; major rotamer) δ 170.2, 170.0, 162.8, 160.2, 136.2 (d, J = 3.3 Hz), 135.8 (d, J = 3.3 Hz), 128.5 (d, J = 8.2 Hz), 127.9 (d, J = 8.2 Hz), 115.1 (d, J = 21.4 Hz), 114.8 (d, J = 21.4 Hz), 54.8, 49.0, 29.6, 27.1, 21.8, 21.3, 17.3, 15.4; HRMS m/z $[M + H]^+$ calcd for $C_{11}H_{15}FNO$ 196.1132, found 196.1131.

***N*-(1-(4-Chlorophenyl)ethyl)-*N*-methylacetamide (5o).** Silica gel chromatography (3:1 diethyl ether/chloroform) yielded 263 mg (79% yield) of *N*-(1-(4-chlorophenyl)ethyl)-*N*-methylacetamide as a yellow oil: TLC R_f = 0.35 (3:1 ether/chloroform); ^{1}H NMR (400 MHz, $CDCl_3$; major rotamer) δ 7.35−7.16 (m, 4H), 6.04 (q, J = 7.1 Hz, 1H), 2.65 (s, 3H), 2.13 (s, 3H), 1.46 (d J = 7.1 Hz, 3H); ^{13}C NMR (100 MHz, $CDCl_3$; major rotamer) δ 170.5, 170.2, 139.0, 138.6, 133.1, 132.8, 128.6, 128.4, 120.3, 127.6, 55.0, 49.2, 29.9, 27.4, 21.5, 17.4, 15.4; HRMS m/z $[M + H]^+$ calcd for $C_{11}H_{15}ClNO$ 212.0837, found 212.0841.

***N*-Methyl-*N*-(1-(3-(trifluoromethyl)phenyl)ethyl)acetamide (6o).** Silica gel chromatography (2:1 EtOAc/hexanes) yielded 304 mg (47% yield) of *N*-methyl-*N*-(1-(3-(trifluoromethyl)phenyl)ethyl)-acetamide as a clear oil: TLC R_f = 0.4 (2:1 hexanes/EtOAc); ^{1}H NMR (400 MHz, $CDCl_3$; major rotamer) ^{1}H NMR δ 7.50−7.41 (m), 7.41 (s), 6.12 (q, J = 7.1 Hz, 1H), 2.68 (s, 3H), 2.16 (s, 3H), 1.52 (q, J = 7.1 Hz, 3H); ^{13}C NMR (100 MHz, $CDCl_3$; major rotamer) δ 170.2, 141.6, 130.3, 130.2 (q, J_{C-F} = 32.1 Hz), 128.5, 125.0, 123.5 (q, J_{C-F} = 3.7 Hz), 123.2 (q, J_{C-F} = 3.7 Hz), 49.2, 29.6, 21.6, 15.0; HRMS m/z $[M + H]^+$ calcd for $C_{12}H_{15}F_3NO$ 246.1100, found 246.1112.

***N*-Methyl-*N*-(1-(4-(trifluoromethyl)phenyl)ethyl)acetamide (7o).** Silica gel chromatography (2:1 EtOAc/hexanes) yielded 345 mg (53% yield) of *N*-methyl-*N*-(1-(4-(trifluoromethyl)phenyl)ethyl)-acetamide as a yellow oil: TLC R_f = 0.4 (2:1 hexanes/EtOAc); ^{1}H NMR (400 MHz, $CDCl_3$; major rotamer) ^{1}H NMR δ 7.63−7.58 (m), 7.41−7.35 (m), 7.26, 6.11 (q, J = 7.1 Hz, 1H), 2.68 (s, 3H), 2.15 (s, 3H), 1.51 (d, J = 7.1 Hz, 3H); ^{13}C NMR (100 MHz, $CDCl_3$; major rotamer) δ 170.5, 170.2, 144.9, 144.4, 129.5, 129.2, 128.9, 128.6 (q, J = 31.12), 127.3, 126.6, 125.4, 125.0, 122.6, 122.4, 119.9, 117.7, 55.2, 49.5, 29.9, 27.4, 21.8, 21.3, 17.2, 15.2; HRMS m/z $[M + H]^+$ calcd for $C_{12}H_{15}F_3NO$ 246.1100, found 246.1114.

***N*-Methyl-*N*-(1-(3-nitrophenyl)ethyl)acetamide (8o).** Silica gel chromatography (2:1 EtOAc/hexanes) yielded 334 mg (31% yield) of *N*-methyl-*N*-(1-(3-nitrophenyl)ethyl)acetamide as a yellow oil: TLC R_f = 0.15 (2:1 hexanes/EtOAc); ^{1}H NMR (400 MHz, $CDCl_3$; major rotamer) δ 8.12−8.13 (m, 2H), 7.64 (m, 1H), 7.53 (m, 1H), 6.13 (q, J = 7 Hz, 1H), 2.74 (s, 3H), 2.18 (s, 3H), 1.57 (d, J = 7 Hz, 3H); ^{13}C NMR (100 MHz, $CDCl_3$; major rotamer) δ 170.9, 170.5, 148.4, 143.3, 142.8, 133.7, 132.6, 129.9, 128.5, 122.7, 122.3, 121.7, 121.4, 55.3, 49.7, 30.3, 27.7, 22.2, 21.7, 17.6, 15.7; HRMS m/z $[M + H]^+$ calcd for $C_{11}H_{15}N_2O_3$ 233.1077, found 223.1077.

4-(1-(*N*-Methylacetamido)ethyl)pyridin-1-ium 4-Methylbenzenesulfonate (11o). This compound was generated in situ by addition of TsOH monohydrate (2.8 mg, 1.1 equivalents) to 1 mL of a 15 mM solution of **10o** in $CDCl_3$: ^{1}H NMR (400 MHz, $CDCl_3$; major rotamer) δ 8.85 (d, J = 6.3 Hz, 2H), 7.78 (d, J = 6.3 Hz, 2H), 7.72 (d, J = 8.0 Hz, 2H), 7.12 (d, J = 8.0 Hz, 2H), 7.00 (broad, 1H), 5.84 (q, J = 7.4 Hz, 1H), 2.80 (s, 3H), 2.31 (s, 3H), 2.12 (s, 3H), 1.51 (q, J = 7.3 Hz, 3H); ^{13}C NMR (100 MHz, $CDCl_3$; major rotamer) δ 171.6, 162.3, 142.2, 141.8, 140.1, 128.9, 125.8, 124.1, 51.3, 31.6, 21.9, 21.2, 15.6.

***N*-Methyl-*N*-(3-nitrobenzyl)acetamide (12o).** Aqueous workup yielded 283 mg (54% yield) of *N*-methyl-*N*-(3-nitrobenzyl)acetamide as a yellow oil with sufficient purity such that column chromatography was not required: TLC R_f = 0.45 (95:5 chloroform/2-propanol); ^{1}H NMR (400 MHz, $CDCl_3$; major rotamer) δ 8.14 (d, J=8.1, 1H), 8.08 (s, 1H), 7.41 (d, J = 8.9, 2H), 7.61 (d, J = 7.7, 1H), 7.51 (t, J = 7.9, 1H), 4.68 (s, 2H), 3.00 (s, 3H), 3.00 (s, 3H), 2.20 (s, 3H); ^{13}C NMR (100 MHz, $CDCl_3$; major rotamer) δ 170.8, 148.2, 139.6, 133.9, 129.5, 122.3, 122.2, 50.0, 35.8, 21.5; HRMS m/z $[M + H]^+$ calcd for $C_{10}H_{13}N_2O_3$ 209.0921, found 209.0922.

***N*-Methyl-*N*-(1-(*o*-tolyl)ethyl)acetamide (14o).** Silica gel chromatography (2:1 EtOAc/hexanes) yielded 275 mg (54% yield) of *N*-methyl-*N*-(1-(*o*-tolyl)ethyl)acetamide as an amorphous white solid: TLC R_f = 0.40 (2:1 hexanes/EtOAc); ^{1}H NMR (400 MHz, $CDCl_3$; major rotamer) δ 7.29−7.33 (m, 1H), 7.13−7.21 (m, 3H), 5.97 (q, J = 6.9 Hz, 1H), 2.51 (s, 3H), 2.20 (s, 3H), 2.07 (s, 3H), 1.44 (d, J = 6.9 Hz); ^{13}C NMR (100 MHz, $CDCl_3$; major rotamer) δ 169.2, 137.5, 137.2, 130.1, 127.1, 126.4, 125.2, 48.0, 29.6, 21.6, 18.5, 15.2; HRMS m/z $[M + H]^+$ calcd for $C_{12}H_{18}NO$ 192.1383, found 192.1393.

***N*-Methyl-*N*-(1-(naphthalen-1-yl)ethyl)acetamide (15o).** Aqueous workup yielded 366 mg (17% yield) of *N*-methyl-*N*-(1-(naphthalen-1-yl)ethyl)acetamide as an amorphous white solid with sufficient purity such that column chromatography was not required: TLC R_f = 0.35 (2:1 hexanes/EtOAc); ^{1}H NMR (400 MHz, $CDCl_3$; major rotamer) δ 8.03 (d, J = 8.2 Hz, 1H), 7.84 (d, J = 8.2 Hz, 1H), 7.80 (d, J = 8.1 Hz, 1H), 7.43−7.53 (m, 4H), 6.61 (q, J = 6.8 Hz, 1H), 2.47 (s, 3H), 2.09 (s, 3H), 1.60 (d, J = 6.8 Hz, 3H); ^{13}C NMR (100 MHz, $CDCl_3$; major rotamer) δ 169.9, 136.0, 133.7, 131.3, 128.6, 128.5, 126.7, 125.9, 124.8, 124.8, 123.8, 47.6, 29.9, 22.3, 15.7; HRMS m/z $[M + H]^+$ calcd for $C_{15}H_{18}NO$ 228.1383, found 228.1387.

***N*-(1-(4-Methoxyphenyl)ethyl)-*N*-methylethanethioamide (1s).** Silica gel chromatography (3:1 hexanes/EtOAc) yielded 106 mg (41% yield) of *N*-(1-(4-methoxyphenyl)ethyl)-*N*-methylethanethioamide as a white crystalline solid: mp 75 °C; TLC R_f = 0.5 (2:1 hexanes/EtOAc); ^{1}H NMR (400 MHz, $CDCl_3$; major rotamer) δ 7.25 (AA′BB′, J = 9.0 Hz, 2H), 7.18 (q, J = 7.2, 1H), 6.88 (AA′BB′ J = 8.8, 2H), 3.81 (s, 3H), 2.84 (s, 3H), 2.67 (s, 3H), 1.54 (d, J = 7.0, 3H); ^{13}C NMR (100 MHz, $CDCl_3$; major rotamer) δ 199.5, 159.0, 131.0, 128.2, 113.8, 57.8, 55.1, 33.5, 33.1, 14.4; HRMS m/z $[M + H]^+$ calcd for $C_{12}H_{18}NOS$ 224.1104, found 224.1104.

***N*-Methyl-*N*-(1-(*p*-tolyl)ethyl)ethanethioamide (2s).** Silica gel chromatography (4:1 hexanes/EtOAc) yielded 70 mg (30% yield) of *N*-methyl-*N*-(1-(*p*-tolyl)ethyl)ethanethioamide as an amorphous white solid: TLC R_f = 0.5 (4:1 hexanes/EtOAc); ^{1}H NMR (400 MHz, $CDCl_3$; major rotamer) δ ^{1}H NMR 7.24−7.15 (m), 7.10−7.08 (m), 2.68 (s, 3H), 2.85 (s, 3H), 2.34 (s, 3H), 1.55 (d, J = 7.1 Hz, 3H); ^{13}C NMR (100 MHz, $CDCl_3$; major rotamer) δ 200.1, 199.2, 138.1, 137.7, 136.2, 135.7, 129.9, 129.6, 127.2, 126.5, 59.7, 58.5, 37.0, 34.1, 33.5, 32.7, 21.3, 21.2, 17.2, 14.7; HRMS m/z $[M + H]^+$ calcd for $C_{12}H_{18}NS$ 208.1154, found 208.1165.

***N*-Methyl-*N*-(1-phenylethyl)ethanethioamide (3s).** Silica gel chromatography (3:1 hexanes/EtOAc) yielded 83 mg (22% yield) of *N*-methyl-*N*-(1-phenylethyl)ethanethioamide as a green oil: TLC R_f = 0.2 (9:1 Hexanes/EtOAc); ^{1}H NMR (400 MHz, $CDCl_3$; major rotamer) δ 7.43−7.19 (m, 5H; contains q, 1H), 2.86 (s, 3H), 2.69 (s, 3H), 1.57 (d, J = 6.9, 3H); ^{13}C NMR (100 MHz, $CDCl_3$; major rotamer) δ 200.1, 139.0, 128.6, 127.7, 127.0, 58.3, 33.8, 33.1, 14.3; HRMS m/z $[M + H]^+$ calcd for $C_{11}H_{16}NS$ 194.0998, found 194.0941.

***N*-(1-(4-Fluorophenyl)ethyl)-*N*-methylethanethioamide (4s).** Silica gel chromatography (3:1 hexanes/EtOAc) yielded 326 mg (67% yield) of *N*-(1-(4-fluorophenyl)ethyl)-*N*-methylethanethioamide as a yellow amorphous solid: TLC R_f = 0.3 (3:1 hexanes/EtOAc); ^{1}H NMR (400 MHz, $CDCl_3$; major rotamer) ^{1}H NMR δ 7.34−7.30 (m), 7.24 (q, J = 7.1 Hz, 1H), 7.21−7.17 (m), 7.10−7.02 (m), 2.69 (s, 3H0, 2.86 (s, 3H), 1.56 (d, J = 7.1 Hz, 3H); ^{13}C NMR (100 MHz, $CDCl_3$; major rotamer) δ 200.0, 199.0, 163.2, 160.8, 134.7 (d, J = 3.3 Hz), 134.1 (d, J = 3.3 Hz), 128.6 (d, J = 8.2 Hz), 130.0 (d, J = 8.2 Hz), 115.7 (d, J = 21.4 Hz), 115.3 (d, J = 21.4 Hz), 58.9, 57.5, 36.4, 33.6, 33.0, 32.2, 16.9, 14.5; HRMS m/z $[M + H]^+$ calcd for $C_{11}H_{15}FNS$ 212.0904, found 212.0904.

***N*-(1-(4-Chlorophenyl)ethyl)-*N*-methylethanethioamide (5s).** Silica gel chromatography (4:1 hexanes/EtOAc) yielded 90 mg (40% yield) of *N*-(1-(4-chlorophenyl)ethyl)-*N*-methylethanethioamide as a yellow oil: TLC R_f = 0.3 (4:1 hexanes/EtOAc); ^{1}H NMR (400 MHz, $CDCl_3$; major rotamer) ^{1}H NMR δ 7.38−7.13 (m, 4H), 7.23 (q, J = 7.1 Hz, 1H), 2.85 (s, 3H), 2.69 (s, 3H), 1.55 (d, J = 7.1 Hz, 3H); ^{13}C

dx.doi.org/10.1021/jo4014113 | J. Org. Chem. 2013, 78, 11172−11183

NMR (100 MHz, $CDCl_3$; major rotamer) δ 200.7, 199.7, 137.9, 137.3, 134.3, 133.9, 129.4, 129.1, 128.7, 128.0, 59.3, 58.0, 37.0, 34.1, 33.5, 32.7, 17.3, 15.8; HRMS m/z $[M + H]^+$ calcd for $C_{11}H_{15}ClNS$ 226.0608, found 228.0607.

***N*-Methyl-*N*-(1-(3-(trifluoromethyl)phenyl)ethyl)ethanethioamide (6s).** Silica gel chromatography (4:1 hexanes/EtOAc) yielded 35 mg (35% yield) of *N*-methyl-*N*-(1-(3-(trifluoromethyl)-phenyl)ethyl)ethanethioamide as a white amorphous solid: TLC R_f = 0.3 (3:1 hexanes/EtOAc); ^1H NMR (400 MHz, $CDCl_3$; major rotamer) δ 7.47−7.62 (m, 4H), 7.32 (q, J = 7.0 Hz, 1H), 2.89 (s, 3H), 2.71 (s, 3H), 1.61 (d, J = 7.0 Hz, 3H); ^{13}C NMR (100 MHz, $CDCl_3$; major rotamer) δ 200.9, 140.2, 131.2 (q, J_{C-F} = 32.3 Hz), 130.6 (q, J_{C-F} = 1.4 Hz), 129.6, 129.2, 124.6 (q, J_{C-F} = 3.7 Hz), 123.4 (q, J_{C-F} = 3.7 Hz), 57.8, 33.9, 33.1, 14.5; HRMS m/z $[M + H]^+$ calcd for $C_{12}H_{15}F_3NS$ 262.0872, Found 262.0899.

***N*-Methyl-*N*-(1-(4-(trifluoromethyl)phenyl)ethyl)ethanethioamide (7s).** Silica gel chromatography (4:1 hexanes/EtOAc) yielded 52 mg (14% yield) of *N*-methyl-*N*-(1-(4-(trifluoromethyl)-phenyl)ethyl)ethanethioamide as a yellow oil: TLC R_f = 0.6 (2:3 hexanes/EtOAc); ^1H NMR (400 MHz, $CDCl_3$; major rotamer) δ 7.47−7.62 (m, 4H), 7.32 (q, J = 7.0 Hz, 1H), 2.89 (s, 3H), 2.71 (s, 3H), 1.61 (d, J = 7.0 Hz, 3H); ^{13}C NMR (100 MHz, $CDCl_3$; major rotamer) δ 200.9, 143.1, 129.9 (q, J_{C-F} = 32.2 Hz), 127.3, 125.6 (q, J_{C-F} = 3.7 Hz), 125.3, 57.8, 33.9, 33.1, 14.5; HRMS m/z $[M + H]^+$ calcd for $C_{12}H_{15}F_3NS$ 262.0872, found 262.0877.

***N*-Methyl-*N*-(1-(3-nitrophenyl)ethyl)ethanethioamide (8s).** Silica gel chromatography (2:1 hexanes/EtOAc) yielded 37 mg (35% yield) of *N*-methyl-*N*-(1-(3-nitrophenyl)ethyl)ethanethioamide as a white crystalline solid: mp 94 °C; TLC R_f = 0.2 (2:1 hexanes/EtOAc); ^1H NMR (400 MHz, $CDCl_3$; major rotamer) δ 8.13−8.23 (m, 2H), 7.70 (m, 1H), 7.55 (m, 1H), 7.38 (q, J = 7 Hz, 1H), 2.92 (s, 3H), 2.73 (s, 3H), 1.65 (d, J = 7.0 Hz, 3H); ^{13}C NMR (100 MHz, $CDCl_3$; major rotamer) δ 201.4, 141.5, 133.6, 130.2, 129.8, 122.9, 121.5, 57.5, 33.9, 33.2, 14.8; HRMS m/z $[M + H]^+$ calcd for $C_{11}H_{15}N_2O_2S$ 239.0849, found 239.0858.

***N*-Methyl-*N*-(1-(4-nitrophenyl)ethyl)ethanethioamide (9s).** Silica gel chromatography (2:1 hexanes/EtOAc) yielded 112 mg (69% yield) of *N*-methyl-*N*-(1-(4-nitrophenyl)ethyl)ethanethioamide as a yellow crystalline solid: mp 71 °C; TLC R_f = 0.45 (2:1 Hexanes/EtOAc); ^1H NMR (400 MHz, $CDCl_3$; major rotamer) δ 8.23 (d, J = 8.9, 2H), 7.51 (d, J = 8.6, 2H), 2.91 (s, 3H), 2.73 (s, 3H), 1.64 (d, J = 3.4, 3H); ^{13}C NMR (100 MHz, $CDCl_3$; major rotamer) δ 201.3, 147.3, 146.5, 127.7, 123.8, 57.7, 33.9, 32.9, 14.7; HRMS m/z $[M + H]^+$ calcd for $C_{11}H_{15}N_2O_2S$ 239.0849, found 239.0845.

***N*-Methyl-*N*-(3-nitrobenzyl)ethanethioamide (12s).** Aqueous workup yielded 48 mg (45% yield) of *N*-methyl-*N*-(3-nitrobenzyl)-ethanethioamide as a yellow crystalline solid with sufficient purity such that column chromatography was not required: mp 109−110 °C; TLC R_f = 0.3 (2:1 hexanes/EtOAc); ^1H NMR (400 MHz, $CDCl_3$; major rotamer) δ 8.17 (d, J = 8.5, 1H), 8.14 (s, 1H), 7.12 (d, J = 7.8, 1H), 7.54 (t, J = 7.6, 1H), 5.43 (s, 2H), 3.25 (s, 3H), 2.74 (s, 3H); ^{13}C NMR (100 MHz, $CDCl_3$; major rotamer) δ 211.3, 137.6, 133.8, 131.9, 129.8, 122.8, 122.5, 57.6, 39.7, 32.9; HRMS m/z $[M + H]^+$ calcd for $C_{10}H_{13}N_2O_2S$ 225.0692, found 225.0692.

***N*-Methyl-*N*-(4-nitrobenzyl)ethanethioamide (13s).** Silica gel chromatography (3:1 hexanes/EtOAc) yielded 16 mg (10% yield) of *N*-methyl-*N*-(4-nitrobenzyl)ethanethioamide as a yellow crystalline solid: mp 140−141 °C; TLC R_f = 0.3 (2:1 hexanes/EtOAc); ^1H NMR (400 MHz, $CDCl_3$; major rotamer) δ 8.22 (d, J = 8.9, 2H), 7.48 (d, J = 8.9, 2H), 5.43 (s, 2H), 3.24 (s, 3H), 2.76 (s, 3H); ^{13}C NMR (100 MHz, $CDCl_3$; major rotamer) δ 202.1, 142.9, 128.4, 127.0, 124.0, 57.8, 39.7, 32.9; HRMS m/z $[M + H]^+$ calcd for $C_{10}H_{13}N_2O_2S$ 225.0692, found 225.0691.

***N*-Methyl-*N*-(1-(*o*-tolyl)ethyl)ethanethioamide (14s).** Silica gel chromatography (3:1 hexanes/EtOAc) yielded 30 mg (28% yield) of *N*-methyl-*N*-(1-(*o*-tolyl)ethyl)ethanethioamide as a clear oil: TLC R_f = 0.3 (3:1 hexanes/EtOAc); ^1H NMR (400 MHz, $CDCl_3$; major rotamer) δ 7.39 (m, 1H), 7.24−7.27 (m, 3H), 6.83 (q, J = 6.9 Hz, 1H), 2.75 (s, 3H), 2.64 (s, 3H), 2.22 (s, 3H), 1.57 (d, J = 6.9 Hz, 3H); ^{13}C NMR (100 MHz, $CDCl_3$; major rotamer) δ 198.6, 138.3, 137.1, 130.8, 128.0, 127.0, 126.0, 57.5, 34.0, 33.1, 19.4, 13.9; HRMS m/z $[M + H]^+$ calcd for $C_{12}H_{18}NS$ 208.1154, found 208.1153.

***N*-Methyl-*N*-(1-(naphthalen-1-yl)ethyl)ethanethioamide (15s).** Silica gel chromatography (4:1 hexanes/EtOAc) yielded 30 mg (28% yield) of *N*-methyl-*N*-(1-(naphthalen-1-yl)ethyl)-ethanethioamide as an off-white amorphous solid: TLC R_f = 0.3 (4:1 hexanes/EtOAc); ^1H NMR (400 MHz, $CDCl_3$; major rotamer) δ 8.00 (d, J = 8.3 Hz, 1H), 7.86 (m, 2H), 7.48−7.60 (m, 4H), 7.41 (q, J = 6.8 Hz, 1H), 2.67 (s, 3H), 2.64 (s, 3H), 1.71 (d, J = 6.8 Hz, 3H); ^{13}C NMR (100 MHz, $CDCl_3$; major rotamer) δ 198.7, 135.4, 133.7, 132.1, 129.1, 128.6, 127.2, 126.1, 125.2, 125.0, 124.2, 56.8, 33.9, 33.3, 14.0; HRMS m/z $[M + H]^+$ calcd for $C_{15}H_{18}NS$ 244.1154, found 244.1155.

Computational Methods. All electronic structure calculations were performed using Gaussian09 (revision C.01).[72] Geometry optimizations, including relaxed potential energy scans, were conducted at the B3LYP/6-31+G(d) level of theory. Potential energy scans were conducted by iteratively fixing the dihedral angle of interest in 5° increments, followed by minimization of the resulting structure. For fully optimized *cis* and *trans* models, frequency calculations were performed at the same level of theory to ensure that no imaginary frequencies were found. The reported energy values are uncorrected SCF energies. NBO analyses of optimized structures were conducted using NBO version 5.9.[73]

■ ASSOCIATED CONTENT

Ⓢ Supporting Information

Characterization data for model peptoids and thiopeptoids and computational data. This material is available free of charge via the Internet at http://pubs.acs.org.

■ AUTHOR INFORMATION

Corresponding Author

*E-mail: bgorske@bowdoin.edu.

Notes

The authors declare no competing financial interest.

■ ACKNOWLEDGMENTS

This research was supported by an award from Research Corporation for Science Advancement. Support for the LCMS instrumentation at Bowdoin College by the NSF (CHE-1126657) is gratefully acknowledged. Portions of this research were conducted using the Phoenix Cluster at the University of Wisconsin—Madison, which is supported in part by National Science Foundation Grant No. CHE-0840494. Z.S.B. and A.M.C. acknowledge the Howard Hughes Medical Institute Undergraduate Science Program for funding. We thank Professor Clark Landis for contributive discussions and access to computational resources at the University of Wisconsin—Madison.

■ REFERENCES

(1) Seebach, D.; Gardiner, J. *Acc. Chem. Res.* **2008**, *41*, 1366−1375.
(2) Miller, S. M.; Simon, R. J.; Ng, S.; Zuckermann, R. N.; Kerr, J. M.; Moos, W. H. *Bioorg. Med. Chem. Lett.* **1994**, *4*, 2657−2662.
(3) Simon, R. J.; Kania, R. S.; Zuckermann, R. N.; Huebner, V. D.; Jewell, D. A.; Banville, S.; Ng, S.; Wang, L.; Rosenberg, S.; Marlowe, C. K.; Spellmeyer, D. C.; Tan, R.; Frankel, A. D.; Santi, D. V.; Cohen, F. E.; Bartlett, P. A. *Proc. Nat. Acad. Sci. U.S.A.* **1992**, *89*, 9367−9371.
(4) Zuckermann, R. N.; Kerr, J. M.; Kent, S. B. H.; Moos, W. H. *J. Am. Chem. Soc.* **1992**, *114*, 10646−10647.
(5) Nguyen, J. T.; Turck, C. W.; Cohen, F. E.; Zuckermann, R. N.; Lim, W. A. *Science* **1998**, *282*, 2088−2092.
(6) Hamuro, Y.; Geib, S.; Hamilton, A. *J. Am. Chem. Soc.* **1997**, *119*, 10587−10593.
(7) Cheng, R. P.; Gellman, S. H.; DeGrado, W. F. *Chem. Rev.* **2001**, *101*, 3219−3232.

(8) Appella, D. H.; Christianson, L. A.; Karle, I. L.; Powell, D. R.; Gellman, S. H. *J. Am. Chem. Soc.* **1996**, *118*, 13071−13072.
(9) Appella, D. H.; Christianson, L. A.; Klein, D. A.; Powell, D. R.; Huang, X.; Barchi, J. J.; Gellman, S. H. *Nature* **1997**, *387*, 381−384.
(10) Stephens, O. M.; Kim, S.; Welch, B. D.; Hodsdon, M. E.; Kay, M. S.; Schepartz, A. *J. Am. Chem. Soc.* **2005**, *127*, 13126−13127.
(11) Huc, I. *Eur. J. Org. Chem.* **2004**, 17−29.
(12) Hill, D. J.; Mio, M. J.; Prince, R. B.; Hughes, T. S.; Moore, J. S. *Chem. Rev.* **2001**, *101*, 3893−4012.
(13) Berl, V.; Huc, I.; Khoury, R. G.; Krische, M. J.; Lehn, J.-M. *Nature* **2000**, *407*, 720−723.
(14) Gellman, S. H. *Acc. Chem. Res.* **1998**, *31*, 173−180.
(15) Hamper, B. C.; Kolodziej, S. A.; Scates, A. M.; Smith, R. G.; Cortez, E. *J. Org. Chem.* **1998**, *63*, 708−718.
(16) Norgren, A. S.; Zhang, S.; Arvidsson, P. I. *Org. Lett.* **2006**, *8*, 4533−4536.
(17) Olsen, C. A.; Bonke, G.; Vedel, L.; Adsersen, A.; Witt, M.; Franzyk, H.; Jaroszewski, J. W. *Org. Lett.* **2007**, *9*, 1549−1552.
(18) Roy, O.; Faure, S.; Thery, V.; Didierjean, C.; Taillefumier, C. *Org. Lett.* **2008**, *10*, 921−924.
(19) Olsen, C. A. *Biopolymers* **2011**, *96*, 561−566.
(20) Gibson, C.; Goodman, S. L.; Hahn, D.; Hölzemann, G.; Kessler, H. *J. Org. Chem.* **1999**, *64*, 7388−7394.
(21) Sarma, B. K.; Yousufuddin, M.; Kodadek, T. *Chem. Commun.* **2011**, *47*, 10590−10592.
(22) Armand, P.; Kirshenbaum, K.; Falicov, A.; Dunbrack, R. L.; Dill, K. A.; Zuckermann, R. N.; Cohen, F. E. *Fold. Des.* **1997**, *2*, 369−375.
(23) Kirshenbaum, K.; Barron, A. E.; Goldsmith, R. A.; Armand, P.; Bradley, E. K.; Truong, K. T.; Dill, K. A.; Cohen, F. E.; Zuckermann, R. N. *Proc. Nat. Acad. Sci. U.S.A.* **1998**, *95*, 4303−4308.
(24) Sanborn, T. J.; Wu, C. W.; Zuckermann, R. N.; Barron, A. E. *Biopolymers* **2001**, *63*, 12−20.
(25) Wu, C. W.; Kirshenbaum, K.; Sanborn, T. J.; Patch, J. A.; Huang, K.; Dill, K. A.; Zuckermann, R. N.; Barron, A. E. *J. Am. Chem. Soc.* **2003**, *125*, 13525−13530.
(26) Shin, S. B. Y.; Yoo, B.; Todaro, L. J.; Kirshenbaum, K. *J. Am. Chem. Soc.* **2007**, *129*, 3218−3225.
(27) Shah, N. H.; Butterfoss, G. L.; Nguyen, K.; Yoo, B.; Bonneau, R.; Rabenstein, D. L.; Kirshenbaum, K. *J. Am. Chem. Soc.* **2008**, *130*, 16622−16632.
(28) Stringer, J. R.; Crapster, J. A.; Guzei, I. A.; Blackwell, H. E. *J. Org. Chem.* **2010**, *75*, 6068.
(29) Jordan, P. A.; Paul, B.; Butterfoss, G. L.; Renfrew, P. D.; Bonneau, R.; Kirshenbaum, K. *Biopolymers* **2011**, *96*, 617−626.
(30) Crapster, J. A.; Stringer, J. R.; Guzei, I. A.; Blackwell, H. E. *Biopolymers* **2011**, *96*, 604−616.
(31) Stringer, J. R.; Crapster, J. A.; Guzei, I. A.; Blackwell, H. E. *J. Am. Chem. Soc.* **2011**, *133*, 15559−15567.
(32) Zuckermann, R. N.; Martin, E. J.; Spellmeyer, D. C.; Stauber, G. B.; Shoemaker, K. R.; Kerr, J. M.; Figliozzi, G. M.; Goff, D. A.; Siani, M. A.; Simon, R. J.; Banville, S. C.; Brown, E. G.; Wang, L.; Richter, L. S.; Moos, W. H. *J. Med. Chem.* **1994**, *37*, 2678−2685.
(33) Huang, C.-Y.; Uno, T.; Murphy, J. E.; Lee, S.; Hamer, J. D.; Escobedo, J. A.; Cohen, F. E.; Radhakrishnan, R.; Dwarki, V.; Zuckermann, R. N. *Chem. Biol.* **1998**, *5*, 345−354.
(34) Brown, N. J.; Johansson, J.; Barron, A. E. *Acc. Chem. Res.* **2008**, *41*, 1409−1417.
(35) Labuda, L. P.; Pushechnikov, A.; Disney, M. D. *ACS Chem. Biol.* **2009**, *4*, 299−307.
(36) Kapoor, R.; Eimerman, P. R.; Hardy, J. W.; Cirillo, J. D.; Contag, C. H.; Barron, A. E. *Antimicrob. Agents Chemother.* **2011**, *55*, 3058−3062.
(37) Patch, J. A.; Barron, A. E. *J. Am. Chem. Soc.* **2003**, *125*, 12092−12093.
(38) Lim, H.-S.; Archer, C. T.; Kodadek, T. *J. Am. Chem. Soc.* **2007**, *129*, 7750−7751.
(39) Maayan, G.; Ward, M. D.; Kirshenbaum, K. *Proc. Nat. Acad. Sci. U.S.A.* **2009**, *106*, 13679−13684.
(40) Vollrath, S. B. L.; Hu, C.; Bräse, S.; Kirshenbaum, K. *Chem. Commun.* **2013**, *49*, 2317−2319.
(41) Sanii, B.; Kudirka, R.; Cho, A.; Venkateswaran, N.; Olivier, G. K.; Olson, A. M.; Tran, H.; Harada, R. M.; Tan, L.; Zuckermann, R. N. *J. Am. Chem. Soc.* **2011**, *133*, 20808−20815.
(42) Lee, B.-C.; Chu, T. K.; Dill, K. A.; Zuckermann, R. N. *J. Am. Chem. Soc.* **2008**, *130*, 8847−8855.
(43) Lee, B.-C.; Zuckermann, R. N.; Dill, K. A. *J. Am. Chem. Soc.* **2005**, *127*, 10999−11009.
(44) Robinson, D. B.; Buffleben, G. M.; Langham, M. E.; Zuckermann, R. N. *Biopolymers* **2011**, *96*, 669−678.
(45) Wu, C. W.; Sanborn, T. J.; Zuckermann, R. N.; Barron, A. E. *J. Am. Chem. Soc.* **2001**, *123*, 2958−2963.
(46) Wu, C. W.; Seurynck, S.; Lee, K.; Barron, A. E. *Chem. Biol.* **2003**, *10*, 1057−1063.
(47) Huang, K.; Wu, C. W.; Sanborn, T. J.; Patch, J. A.; Kirshenbaum, K.; Zuckermann, R. N.; Barron, A. E.; Radhakrishnan, I. *J. Am. Chem. Soc.* **2006**, *128*, 1733−1738.
(48) Armand, P.; Kirshenbaum, K.; Goldsmith, R. A.; Farr-Jones, S.; Barron, A. E.; Truong, K. T.; Dill, K. A.; Mierke, D. F.; Cohen, F. E.; Zuckermann, R. N.; Bradley, E. K. *Proc. Nat. Acad. Sci. U.S.A.* **1998**, *95*, 4309−4314.
(49) Gorske, B. C.; Blackwell, H. E. *J. Am. Chem. Soc.* **2006**, *128*, 14378−14387.
(50) Fowler, S. A.; Luechapanichkul, R.; Blackwell, H. E. *J. Org. Chem.* **2009**, *74*, 1440−1449.
(51) Fowler, S. A.; Blackwell, H. E. *Org. Biomol. Chem.* **2009**, *7*, 1508−1524.
(52) Vaz, B.; Brunsveld, L. *Org. Biomol. Chem.* **2008**, *6*, 2988.
(53) Gorske, B. C.; Bastian, B. L.; Geske, G. D.; Blackwell, H. E. *J. Am. Chem. Soc.* **2007**, *129*, 8928−8929.
(54) Gorske, B. C.; Stringer, J. R.; Bastian, B. L.; Fowler, S. A.; Blackwell, H. E. *J. Am. Chem. Soc.* **2009**, *131*, 16555−16567.
(55) Hinderaker, M. P.; Raines, R. T. *Protein Sci.* **2003**, *12*, 1188−1194.
(56) Caumes, C.; Roy, O.; Faure, S.; Taillefumier, C. *J. Am. Chem. Soc.* **2012**, *134*, 9553−9556.
(57) Laursen, J. S.; Engel-Andreasen, J.; Fristrup, P.; Harris, P.; Olsen, C. A. *J. Am. Chem. Soc.* **2013**, *135*, 2835−2844.
(58) Choudhary, A.; Gandla, D.; Krow, G. R.; Raines, R. T. *J. Am. Chem. Soc.* **2009**, *131*, 7244−7246.
(59) Hara, T.; Durell, S. R.; Myers, M. C.; Appella, D. H. *J. Am. Chem. Soc.* **2006**, *128*, 1995−2004.
(60) Lee, M. M.; Pushechnikov, A.; Disney, M. D. *ACS Chem. Biol.* **2009**, *4*, 345−355.
(61) Hoffmann, R. W. *Chem. Rev.* **1989**, *89*, 1841−1860.
(62) Bhattacharyya, R.; Chakrabarti, P. *J. Mol. Biol.* **2003**, *331*, 925−940.
(63) Guo, H.; Beahm, R. F.; Guo, H. *J. Phys. Chem. B* **2004**, *108*, 18065−18072.
(64) Bhadbhade, M. M.; Kishore, R. *Biopolymers* **2012**, *97*, 73−82.
(65) Hansch, C.; Leo, A.; Taft, R. *Chem. Rev.* **1991**, *91*, 165−195.
(66) Roy, O.; Caumes, C.; Esvan, Y.; Didierjean, C.; Faure, S.; Taillefumier, C. *Org. Lett.* **2013**, *15*, 2246−2249.
(67) Glendening, E. D.; Landis, C. R.; Weinhold, F. *WIREs Comput. Mol. Sci.* **2012**, *2*, 1−42.
(68) Satonaka, H.; Abe, K.; Hirota, M. *Bull. Chem. Soc. Jpn.* **1988**, *61*, 2031−2037.
(69) Marques, M. P. M.; Amorim da Costa, A. M.; Ribeiro-Claro, P. J. A. *J. Phys. Chem. A* **2001**, *105*, 5292−5297.
(70) Ratajczyk, T.; Czerski, I.; Kamienska-Trela, K.; Szymanski, S.; Wojcik, J. *Angew. Chem., Int. Ed. Engl.* **2005**, *44*, 1230−1232.
(71) Newberry, R. W.; Vanveller, B.; Guzei, I. A.; Raines, R. T. *J. Am. Chem. Soc.* **2013**, *135*, 7483−7846.
(72) Frisch, M. J.; Trucks, G. W.; Schlegel, H. B.; Scuseria, G. E.; Robb, M. A.; Cheeseman, J. R.; Scalmani, G.; Barone, V.; Mennucci, B.; Petersson, G. A.; Nakatsuji, H.; Caricato, M.; Li, X.; Hratchian, H. P.; Izmaylov, A. F.; Bloino, J.; Zheng, G.; Sonnenberg, J. L.; Hada, M.; Ehara, M.; Toyota, K.; Fukuda, R.; Hasegawa, J.; Ishida, M.; Nakajima,

T.; Honda, Y.; Kitao, O.; Nakai, H.; Vreven, T.; Montgomery, J. A., Jr.; Peralta, J. A.; Ogliaro, J. E.; Bearpark, M.; Heyd, J. J.; Brothers, E.; Kudin, K. N.; Staroverov, V. N.; Kobayashi, R.; Normand, J.; Raghavachari, K.; Rendell, A.; Burant, J. C.; Iyengar, S. S.; Tomasi, J.; Cossi, M.; Rega, N.; Millam, J. M.; Klene, M.; Knox, J. E.; Cross, J. B.; Bakken, V.; Adamo, C.; Jaramillo, J.; Gomperts, R.; Stratmann, R. E.; Yazyev, O.; Austin, A. J.; Cammi, R.; Pomelli, C.; Ochterski, J. W.; Martin, R. L.; Morokuma, K.; Zakrzewski, V. G.; Voth, G. A.; Salvador, P.; Dannenberg, J. J.; Dapprich, S.; Daniels, A. D.; Farkas, Ö.; Foresman, J. B.; Ortiz, J. V.; Cioslowski, J.; Fox, D. J. Gaussian 09, Revision C.01.

(73) Glendening, E. D.; Badenhoop, J. K.; Reed, A. E.; Carpenter, J. E.; Bohmann, J. A.; Morales, C. M.; Weinhold, F. NBO 5.9.